

**Project Title:**

**Theoretical study of interaction between tunneling electrons  
and individual molecules at surfaces**

**Name** : Yousoo Kim, Taketoshi Minato, Emi Minamitani, Jaehoon Jung,  
Ju-Hyung Kim, and Seiji Takemoto  
**Affiliation** :Surface and Interface Science Laboratory,  
Advanced Science Institute, Wako Institute

---

1 . Background and purpose of the project,  
relationship of the project with other projects.

During the past decade, computer simulations based on a quantum mechanics have developed an increasingly important impact on solid-state physics and chemistry and on materials science. In field of material science, the surface chemistry is fundamentally important in many areas, such as molecular electronics, heterogeneous catalyst, fuel cell, etc. The adsorption of molecules onto a surface is a necessary prerequisite to any surface mediated chemical process. Understanding the bonding nature between the molecule and the surface on the basis of the electronic structure is therefore one of the most important issues in this field. The computational methods like density functional theory (DFT) have played a prominent role to elucidate the interaction between the molecule and the surface.

From the theoretical investigation of the adsorbed molecule on surface in combination with STM experiment, we could expect the following research goals; 1) the deep understanding of the chemical/physical properties of an adsorbate on the surface, 2) the fine control of the chemistry on the surface.

2 . Specific usage status of the system and calculation method

We have been studying the molecular adsorption on the well-defined metal surface using computational method in combination with experimental method. In our studies, first-principles simulations have been carried out using the Vienna Ab-initio Simulation Package (VASP) code in the density functional level of theory. The pure DFT methods have been mostly used and the inner electrons are replaced by projector augmented wave pseudopotentials (PAW). The climbing image nudged elastic band method (CI-NEB) was used to determine the transition states which were confirmed by imaginary frequency modes. In most of cases, STM image simulations were performed using Tersoff-Hamann approach. The computational results have been compared with the available experimental result obtained from STM in our group.

We also have been studying the many-body phenomena in molecular adsorption system, in particular the Kondo effect. The characteristic electronic state resulting from the Kondo effect, so-called Kondo singlet state appears as a sharp peak structure (Kondo peak) at the Fermi level in scanning tunneling spectroscopy (STS). In order to simulate the Kondo peak, we build numerical renormalization group code and the STS simulation code based on the Keldysh Green's function method.

3 . Results

**(1) Activation of ultrathin oxide film by interface defect for chemical reaction**

Ultrathin oxide films grown on metal substrate are of great interest not only as supporting materials for chemically active nanoparticles but also as catalysts in the field of heterogeneous catalysis [H.-J. Freund, *Chem. Eur. J.* **16**, 9384 (2010)]. Using STM and DFT calculations, we have demonstrated that the chemical reactivity for water dissociation on an ultrathin MgO film grown on Ag(100) substrate depends greatly on film thickness and is enhanced as compared to that achieved with their bulk counterpart [H.-J. Shin et al., *Nature Mater.* **9**, 442 (2010); J. Jung et al., *Phys. Rev. B* **82**, 085413 (2010)]. Figure 1 clearly indicates that the chemical activity of the ultrathin MgO film is sensitive to film thickness. This implies that catalytic activity on ultrathin MgO films can be controlled by film thickness.

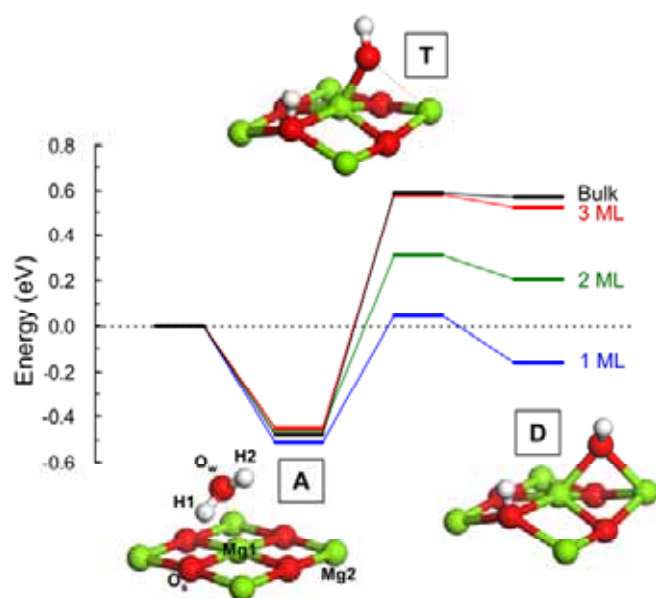


**Figure 1.** (a) The energy diagram (in eV) for the dissociation of a water single molecule on MgO( $n$  ML)/Ag(100) ( $n = 1, 2,$  and  $3$ ) and MgO(100) surfaces and the corresponding atomic structures for  $n = 2$  (H, white; O, red; Mg, green).

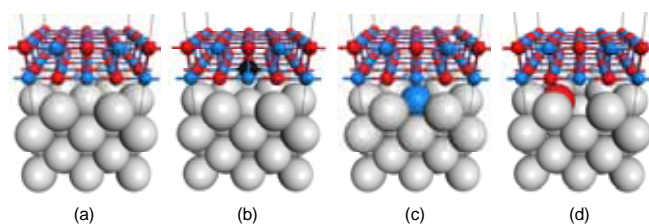


**Figure 2.** Optimized structures for ultrathin MgO film deposited on the Ag(100) substrate with and without the interface defects; (a) non-defect (ND), (b) interface O vacancy ( $int-O_{vac}$ ), (c) interface Mg impurity ( $int-Mg_{imp}$ ), and (d) interface O impurity ( $int-O_{imp}$ ). (Ag, Gray; Mg, blue; O, red; O vacancy, black)

The change of chemical reactivity of ultrathin MgO film depending on the film thickness can be explained by the strengthening of the interaction between the oxide and metal interface layers. This result implies that the artificial manipulation of the local structure at the oxide-metal interface is expected to play a pivotal role in controlling the catalytic activity of oxide film. Therefore, water dissociation on three model systems with defects at the oxide-metal interface of the 2-ML MgO/Ag(100) - an O vacancy, an Mg impurity, or an O impurity (Fig. 2) - has been examined and compared with the case of a MgO film without defects using periodic DFT calculations [J. Jung et al., *J. Am. Chem. Soc.* **133**, 6142 (2011)]. Our results clearly show that such structural imperfections at the interface can improve the chemical reactivity of ultrathin MgO film supported by Ag(100) substrate (Fig. 3). The energy diagram shows that the water molecule is more strongly adsorbed and more easily dissociated on the interface-defective MgO films compared to the non-defective (ND) MgO film. Interestingly, the transition states (**T**) for the  $int-O_{vac}$  and  $int-Mg_{imp}$  locate below 0.0 eV, where the transition state energies,  $E(\mathbf{T})$ , are  $-0.18$  and  $-0.01$  eV, respectively. These cause the barrier heights ( $E_a$ ),  $E(\mathbf{T}) - E(\mathbf{A})$ , to be lowered and, accordingly, to be noticeably reduced by 42 (59) % and 29 (50) % from that of ND MgO film (*bulk MgO*). In company with the exothermic

dissociation energy,  $E(D)$ , for  $int-O_{vac}$  ( $-0.26$  eV) and  $int-Mg_{imp}$  ( $-0.16$  eV), the very low  $E(T)$  implies that water dissociation on the ultrathin MgO film surface with  $int-O_{vac}$  or  $int-Mg_{imp}$  do not require external thermal energy at the level of an individual molecule.

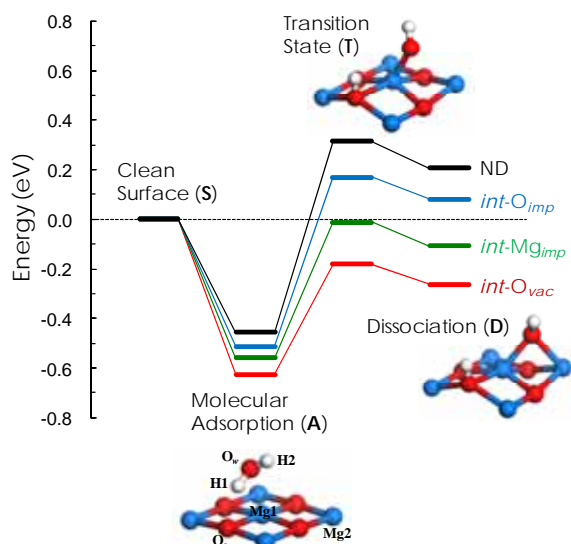


**Figure 3.** Reaction energy diagram (in eV) for the dissociation of a single water molecule on the non-defective (ND) and the defective MgO/Ag(100) surfaces; interface O vacancy ( $int-O_{vac}$ ), interface Mg impurity ( $int-Mg_{imp}$ ), and interface O impurity ( $int-O_{imp}$ ). Non-dissociative adsorption (A), transition state (T), and dissociative adsorption (D) energies are evaluated relative to  $E(H_2O) + E(\text{Substrate}) = 0$  eV. (Mg, blue; O, red; H, white)

This is closely correlated with the accompanying change of charge distribution of the oxide surface due to the accumulation of transferred charge density at the interface (Fig. 4). For the MgO/Ag(100) with defects, the transferred charges are more highly localized at the oxide-metal interface than in the case of ND MgO/Ag(100). The distribution of localized electron density at the interface represents the electronic characteristics of each type of interface defect. The covalent-like interaction between the electrons trapped in  $int-O_{vac}$  and the Ag substrate gives rise to rather a broader charge distribution (Fig. 4b) than other types of

defects (Fig. 4c,d) which show ionic interaction between the MgO layer and impurity atoms embedded in the Ag substrate. Our study reveals that charge localization at the interface strongly redistributes the local charge of the MgO surface (represented by dashed red circles in Fig. 4). Therefore, the adsorption strength of water molecule and the further chemical reactivity of MgO films for water dissociation should be changed as a consequence of the strong charge localization at the oxide-metal interface, as shown in Figure 3. In addition, the chemical reactions on the ultrathin oxide film surface can be tuned by interface defects regardless of the charging of adsorbates. Our study about water dissociation on MgO/Ag(100) not only reveals the potential of an ultrathin oxide film as a catalyst but also opens new vistas for the development of techniques to control and measure the interface structure of oxide film deposited on a metal substrate.

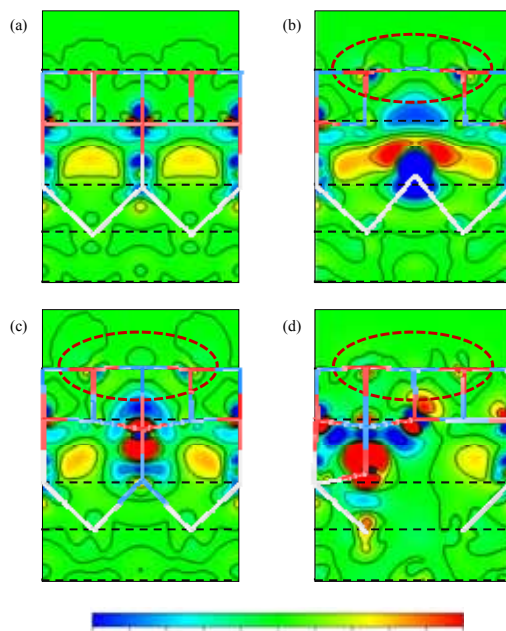


**Figure 4.** The charge density difference maps for non-defective and defective MgO/Ag(100) models; (a) non-defective (ND), (b) interface O vacancy ( $int-O_{vac}$ ), (c) interface Mg impurity ( $int-Mg_{imp}$ ), and (d) interface O impurity ( $int-O_{imp}$ ). The atomic layers are indicated by black dashed lines. The scale is  $\pm 0.003$  e/bohr<sup>3</sup>. The cross-sectional structure is presented by colored solid lines (Ag, Gray; Mg, blue; O, red).

## (2) One-dimensional molecular zippers

Nanometer-scale molecular structures fabricated on solid surfaces have attracted much interest in the effort to produce desired nanostructural patterns for various applications, such as biosensors, molecular electronics, and optoelectronic devices. The conformation of molecular structures on a surface is driven by a subtle balance between molecule-surface and intermolecular interactions, typically hydrogen bonding and/or van der Waals (vdW) interactions. A molecular zipper (MZ) is one of the interesting molecular structures, in which molecules interlock in two directions, along the length of the zip and across it, like a human-made zipper. We have reported isolated 1-D MZs by a combination of hydrogen bonding and vdW interactions between adjacent azobenzene derivatives using STM. In order to understand the electronic and geometric details of observed MZs, we performed the first-principles calculations based on DFT with the 1D periodic boundary condition (PBC).

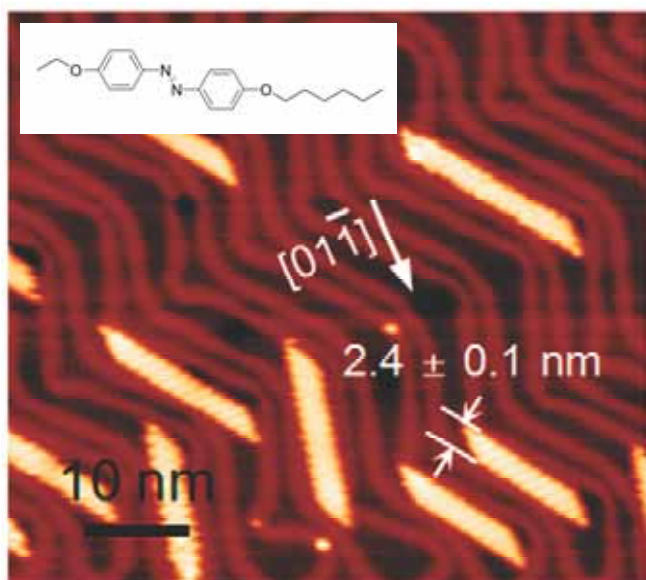


**Figure 5.** STM image of the MZ by EtO-Az-OHx molecules ( $V_s = -1.0$  V,  $I_t = 40$  pA).

Upon deposition on the Au(111) surface, EtO-Az-OHx molecules formed MZs only in fcc regions with an average width of  $2.4 \pm 0.1$  nm, as

shown in Figure 5. Since the width of MZ is slightly larger than that of the hcp region on a reconstructed Au(111) surface, MZ nucleates mainly on the fcc regions.

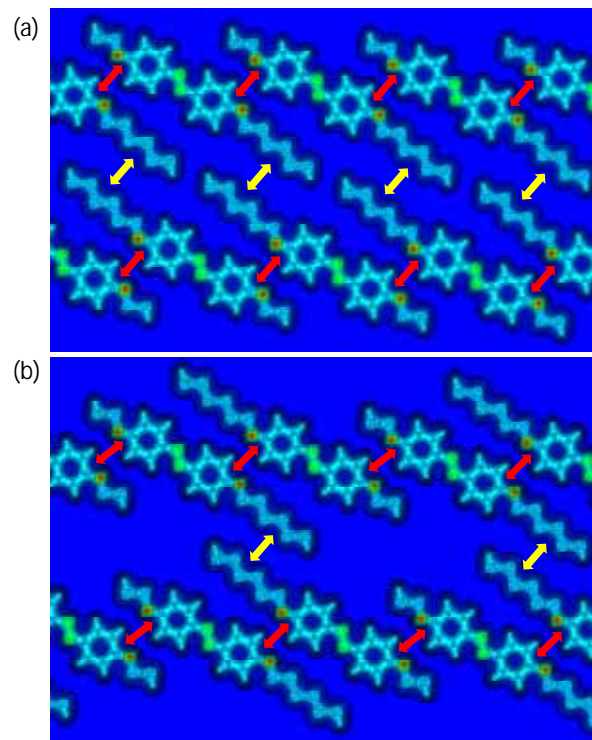


**Figure 6.** Electron densities of (a) “A” and (b) “B”. The red and yellow arrows indicate the intermolecular interaction regions corresponding to hydrogen-bonding and vdW interactions, respectively.

In order to understand the driving force for the EtO-Az-OHx MZ structure, we examined several MZ structures and compared their stability using DFT calculations. Considering two intermolecular interactions (hydrogen bonding and vdW interactions) and the symmetry of the molecular structure, only two kinds of molecular MZs are possible (designated “A” and “B” in Fig. 6). “A” has the structure that we observed in the STM images. Figures 6 also show the calculated electron charge densities of “A” and “B”. The electron density map clearly indicates that the ether oxygen atoms have the highest electron density, providing the hydrogen bonding interactions between two neighboring molecules. This is also supported by the calculated

atomic charges of the EtO-Az-OHx molecule, where the interacting oxygen and hydrogen atoms carry negative (approximately  $-0.3e$ ) and positive (approximately  $+0.1e$ ) charges, respectively. There are two kinds of electronegative elements, *i.e.* O and N, in the molecule. The negative atomic charge of ether O is higher than N by about  $0.1e$ . In addition, the O atoms locate outside compared to the N atoms, which indicates the O atoms more easily participate in the intermolecular hydrogen bonding than the N atoms do. While “A” is composed of only one type of C–H···O hydrogen bonds, namely, “B” has two types of hydrogen bonds, alternately located in each molecular row. Consequently, the alkyl chains in one molecular row of “A” are aligned in the same direction and face each other with the alkyl chains of the neighboring row in an interdigitating pattern. However, those of “B” are alternately positioned within and outside of MZs. Figure 6 indicates the intermolecular interactions using red and yellow arrows to show the hydrogen bonding and vdW interactions, respectively. With this we surmise that the formation of “A” is preferable to “B” because half of the alkyl chains in “B” are unable to take advantage of vdW interaction. The calculated results confirmed that “A” has a higher binding energy by 12 meV per molecule, although DFT calculations do not take full account of dispersion forces between molecules. In addition, the calculated width of “A” is 2.3 nm, which agrees well with the experimentally observed value (Figure 5). The hydrogen bond distances of “A” (2.74~2.75 Å) are shorter than those of “B” (2.74~2.88 Å), which means that the hydrogen-bonding interactions in “A” are stronger than those in “B”. This relative stability of “A” results from the synergetic effect of the hydrogen bonding and vdW interactions. Therefore, we conclude that the formation of 1-D MZs can be achieved through well-balanced intermolecular interactions (*i.e.*, hydrogen bonding and vdW interactions) during molecular deposition on Au(111) surface. Our results provide a novel way of

controlling the width of the MZ by tuning the lengths of the alkyl chains.

### (3) Two dimensional superstructure formation of fluorinated fullerene on Au(111)

Fluorination is an established technique for tuning the electronic and optical properties of organic molecules by stabilizing the energy levels of frontier orbitals. The resulting molecules thus exhibit higher electron affinity (*EA*) than do their original non-fluorinated forms due to the strong electron withdrawal of fluorine atoms. In organic devices such as field effect transistors, the increase in *EA* leads in principle to a decrease in the electron injection barrier at the interface between the molecular film and the metal electrode, yielding n-type semiconducting behavior. A better understanding of the structural and electronic properties of thin films of fluorocarbons deposited on metals is therefore considered essential for further advances in organic electronics.

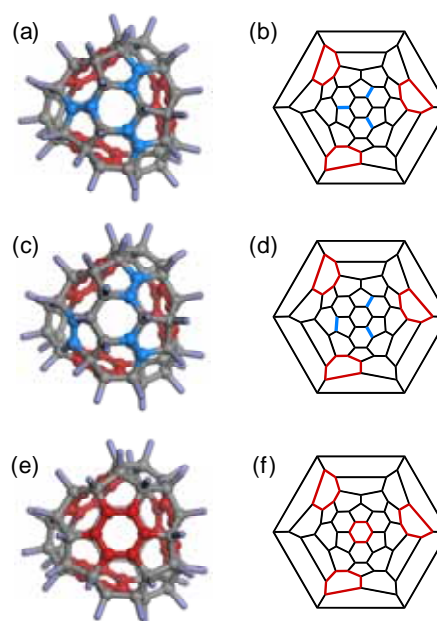


**Figure 7.** Optimized structures (a, c, e) and Schlegel diagrams (b, d, f) for  $C_3$  (a and b),  $C_1$  (c and d), and  $T$  (e and f)  $C_{60}F_{36}$  isomers. Non-fluorinated moieties (phenyl rings and C=C bonds) are colored in red and blue (respectively).

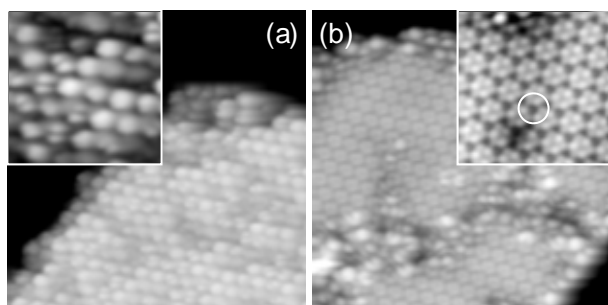


**Figure 8.** STM images ( $20 \times 20 \text{ nm}^2$ ) of  $\text{C}_{60}\text{F}_{36}$  on the Au(111) surface. (a) A  $\text{C}_{60}\text{F}_{36}$  island was formed by depositing molecules onto Au (111) kept at room temperature, producing a number of islands consisting of inhomogeneous regions. (b) A  $\text{C}_{60}\text{F}_{36}$  island created in the same way as in (a) followed by annealing to 370 K for about 5 minutes, resulting in the formation of the homogeneous regions. Insets in (a) and (b) are enlarged images ( $6 \times 6 \text{ nm}^2$ ) of the inhomogeneous and homogeneous regions, respectively. Tunneling parameters in (a) were  $V_{\text{sample}} = 2.4 \text{ V}$  and  $I_t = 0.14 \text{ nA}$ ; in (b)  $V_{\text{sample}} = 2.4 \text{ V}$  and  $I_t = 0.20 \text{ nA}$ .

In this study, we report the successful fabrication and detailed analysis of a well-ordered one-monolayer film made of one of the fluorinated fullerenes,  $\text{C}_{60}\text{F}_{36}$ , on Au(111) using STM and DFT calculations. Although  $\text{C}_{60}\text{F}_{36}$  has three isomers,  $C_3$ ,  $C_1$  and  $T$  (Fig. 7), a well-ordered molecular monolayer consists of only the  $C_3$  isomer, which is reasonably suggested by (i) the highly symmetric and three-fold STM images for the molecules adsorbed on Au(111) shown in Fig. 8, (ii) the difference in orbital distribution of  $C_3$  isomer from those of other isomers (Fig. 9) and (iii) the abundance of the  $C_3$  isomer compared to others ( $C_3:C_1:T = 70:25:5$ ). We found that there is an intermolecular electrostatic interaction between the fluorinated moieties (C-F) and the non-fluorinated moieties ( $\pi$  states of phenyl rings) of adjacent molecules (Fig. 10). This type of C-F... $\pi$  interaction has been reported only for 3D crystals of fluorocarbons.

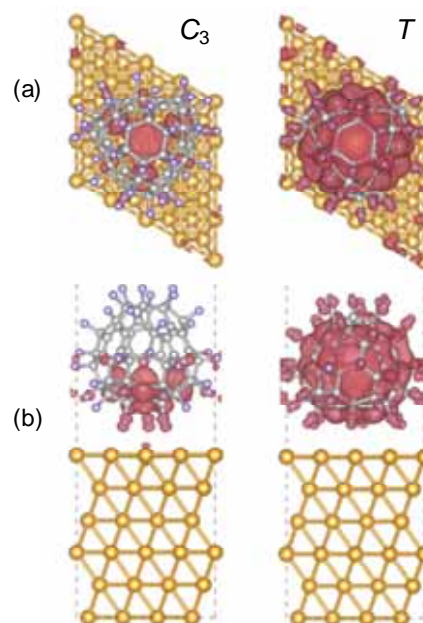


**Figure 9.** Top views (a) and side views (b) of the LUMO distribution of  $C_3$  and  $T$  isomers adsorbed on the top site of Au(111). Iso-surface value is  $0.0015 \text{ e/bohr}^3$ .

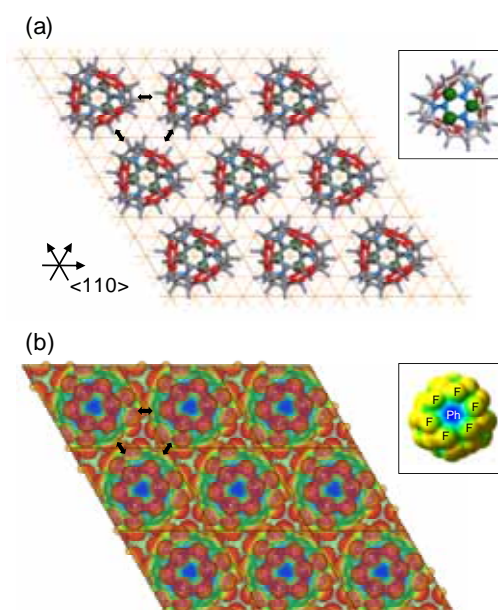


**Figure 10.** (a) ( $4 \times 4$ ) superstructure model for the homogeneous region of the  $\text{C}_{60}\text{F}_{36}$  monolayer on Au(111). Three fluorine atoms at the bottom bonded to Au are emphasized in size and color (green) to clearly show the adsorption sites. Solid yellow lines show the gold lattice. Inset is the bottom view of the single molecule of the  $C_3$  isomer. (b) Calculated electrostatic potential (ESP) distribution of the  $C_3$  isomer. Inset is the ESP calculated in gas phase viewed from the side including a phenyl ring. Color scale from red to blue corresponds to negative to positive. In (a) and (b), C-F... $\pi$  interaction is indicated by black arrows.

Scanning tunneling spectroscopy (STS) revealed that the molecular layer possesses a large bandgap ( $> 5$  eV) with its LUMO much closer to the  $E_F$  than its HOMO, implying that the majority carrier in the film is electrons. The Bader population analysis revealed that  $0.36e$  was transferred from Au(111) to a single  $C_{60}F_{36}$  molecule. This value is larger than that for  $C_{60}/Au(111)$ ,  $0.2e$  per molecule, evaluated using a similar calculation method [L.-L. Wang et al., *Phys. Rev. B* **69**, 165417 (2004)].

Analysis of the LUMO distribution strongly supports the formation of the homogeneous region with only one type of isomer,  $C_3$ , which suggests that the manipulation of the fluorination pattern may allow control over molecular orientation on the substrate. If the separation of isomers can be achieved and established, a complete monolayer of  $C_{60}F_{36}$  on Au electrodes may be feasible. Such a film provides uniform electronic properties with wide band-gap with deep HOMO, and might be technologically relevant, for example, to electron transport layers in organic optoelectronic devices.

#### (4) Density functional theory calculation for magnetism of Fe-Phthalocyanine molecules on Au(111)

The adsorption of magnetic molecules at metal surfaces has long attracted much attention because the bonding interactions between the molecule and the surface strongly influence the molecular magnetism. One of the intriguing phenomena brought about by the coupling of magnetic molecule with metal surface is the Kondo effect. Recently, several works about the adsorption of magnetic molecules at metal surfaces have reported on the formation of the characteristic ground state from the Kondo effect, Kondo singlet state.

We focus on Fe-phthalocyanine (FePc) molecule on

Au(111). To understand the magnetism of FePc on Au(111), it is crucial to unveil the geometric and electronic configurations of FePc on Au(111) and their correlation with the magnetism. However, this is challenging because of the complexity in magnetism of the FePc molecule. The magnetism of FePc has long been controversial both theoretically and experimentally. It has been widely accepted that FePc in the gas phase takes spin triplet ( $S=1$ ) derived from the electronic configuration of  $(3d)^6$ . However, regarding the multiplet state of  $S=1$ , a series of experimental and theoretical investigations have showed inconsistent results. The recent X-ray Absorption Spectroscopy (XAS) and X-ray magnetic circular dichroism (XMCD) works indicate that the plausible multiplet state is  ${}^3E_g$  state represented by  $(d_z^2)^1(d_{xy})^2(d_\pi)^3$ , where  $d_{zx}$  and  $d_{yz}$  orbitals are described as  $d_\pi$ . The previous density functional theory (DFT) calculations show that the exchange correlation functional strongly affects the electron filling of d-orbitals. In addition, DFT+U has recently achieved improvement in the treatment of electron correlation effect in d-electron systems. Thus, it would be beneficial to compare the DFT calculation results for FePc using local density approximation (LDA) with and without +U correction. From this point of view, we carried out the DFT calculation for FePc on Au(111) using LDA and LDA+U.

First, we found the adsorption structure is same in LDA and LDA+U results. Figure 11 shows the stable adsorption structures of the ontop and bridge configurations. The remarkable difference between LDA and LDA+U appears in magnetic moment. In the LDA, the magnetic moment decreases drastically and becomes nearly half of that for the gas phase FePc. On the contrary, in LDA+U, the magnetic moment is close to that of the gas phase FePc. The plausible origin of larger decrease in the magnetic moment for the former is the disadvantages in LDA, which causes the overestimation of the admolecule-substrate bond strength and the

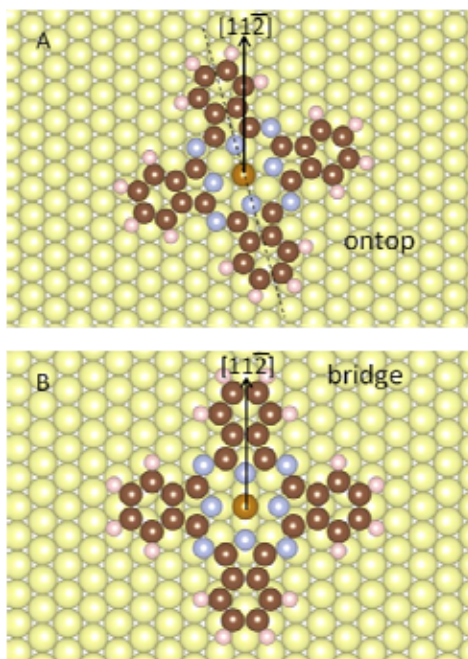


**Figure 11.** Stable adsorption structures in A) ontop and B) bridge configurations.

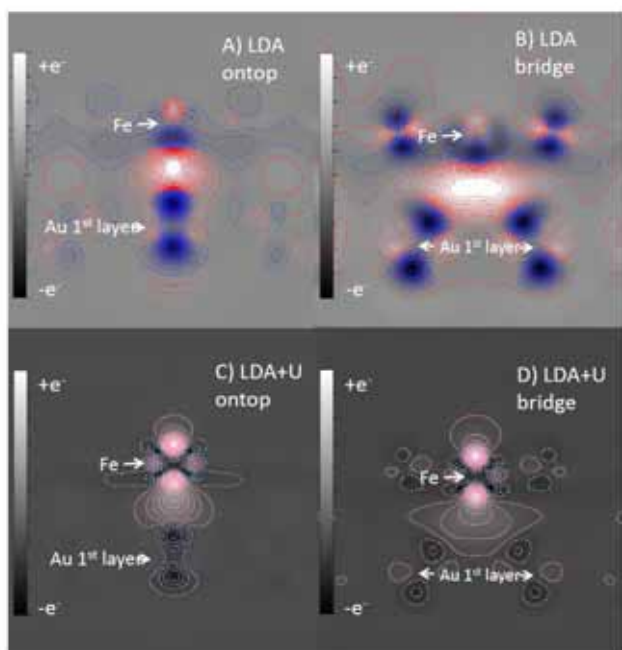


**Figure 12.** Cross sectional views of the differential charge distribution of FePc on Au(111) in the ontop and bridge configurations. The brighter and darker regions show the increase and decrease of electrons, respectively, compared to those of FePc molecule in the gas phase and the Au(111) surface. The red lines are contours in electron increase region and the blue lines are those in electron decrease region.

underestimation of the on-site electron-electron interaction. We found that the charge transfer shown in Fig.12 is different between LDA and LDA+U. In LDA+U, a clear charge decrease region with a cross form appears around the Fe atom. Meanwhile, the charge decrease region around the Fe atom is ambiguous. We concluded that the disadvantages of the LDA treatment causes the overestimation of charge transfer between the Fe atom and Au(111), which results in the underestimation of the residual magnetic moments. This indicates that the LDA+U is more suitable than LDA for the description of the magnetism of FePc on Au(111).

#### 4 . Conclusion

We have tried to examine the molecular behaviors (i.e., chemical reaction, film formation, and Kondo effect) on the surface. First, the way to control the chemical reactivity of the ultrathin MgO film for the water dissociation has been suggested. Our results show that the artificial manipulation of the local structure at the oxide-metal interface is expected to play a pivotal role in controlling the catalytic activity of oxide film. Second, 1-D zipper-type molecular architectures were fabricated using an azobenzene derivative with well-designed functional groups, on an Au(111) surface. The underlying mechanisms for the formation of 1-D molecular zippers can be explained by balanced non-bonding interactions, hydrogen bonding and van der Waals interactions between adjacent molecules. Third, a 2-D superstructure using fluorinated fullerene ( $C_{60}F_{36}$ ) was successfully fabricated on Au(111) and theoretically investigated to reveal the driving force behind the well-ordered film formation. Molecular orientation is determined by the spatial distribution of the frontier molecular orbital with respect to the substrate and the intermolecular  $C-F \cdots \pi$  electrostatic interactions between neighboring

molecules. Finally, we found that the residual magnetic moments calculated by LDA and LDA+U differ from each other in FePc/Au(111), which originates in the difference in the charge transfer between FePc and Au(111).

5 . Schedule and prospect for the future

**(1) Magnetism of molecules on surface -Combining DFT calculations and quantum many-body theories-**

Magnetism of molecules has been investigated intensively due to their potential applications such as single molecular magnets and single molecular spin valves. In order to apply magnetic molecules to realistic devices, we need to place molecules in contact with solid surfaces, i.e., metal electrodes. Depositing molecules on solid surfaces causes various effects such as charge transfer between molecules and surface which changes the electron states of molecules drastically. In addition, in order to discuss the magnetism in adsorbed molecules precisely, we need to treat many-body effects. For this purpose, we try to combine the DFT calculations and quantum many-body theories. Specifically, we construct effective Hamiltonians based on DFT calculations results and solve them using quantum many-body theories.

The target of this research topic is the Kondo effect in adsorbed molecules. In surface systems, the Kondo effect originates in the interaction between the localized spin of the adsorbate and the conduction electrons of the nonmagnetic metal surface. A series of investigations have succeeded to image the Kondo peak of magnetic molecules on a metal surface. However, many points such as considerable variation of Kondo temperature still remain unclear. To unravel and control the molecular Kondo effect, we combine the theoretical methods and STM experiments. In FY2012, we

further explore the Kondo effect in a single molecule on metal surface.

**(2) Controlling chemical reactivity of ultrathin oxide film**

Ultrathin oxide film grown on metal substrate has been a subject of great interest not only as a supporting material for chemically active nanoparticles but also as a catalyst in the field of heterogeneous catalysis, where it provides various ways to control the properties of adsorbates via following factors (See Figure 11): (i) charge transfer between adsorbates and oxide-metal interface, which is closely correlated with the electronic affinity of adsorbate and workfunction reduction, (ii) adhesion between oxide and metal layers with strong polaronic distortion, (iii) film thickness, and (iv) the chemical composition of oxide surface.

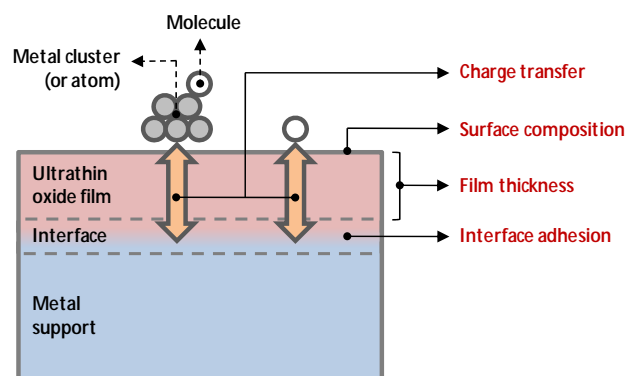


**Figure 11.** Schematic diagram for heterogeneous catalyst using ultrathin oxide film.

Therefore, we will continue our work to find the way for controlling the chemical reactivity using theoretical and experimental studies. From the previous result, we expect that the chemical and physical modification at the oxide-metal interface can open the new way to control the chemical activity of oxide film.

## RICC Usage Report for Fiscal Year 2011

6 . If you wish to extend your account, provide usage situation (how far you have achieved, what calculation you have completed and what is yet to be done) and what you will do specifically in the next usage term.

- Completed researches

(The members registered as the user of RICC system in FY2011 are indicated by underline.)

- (1) Activation of ultrathin oxide film by interface defect for chemical reaction (J. Jung, H.-J. Shin, Y. Kim, and M. Kawai)
- (2) One-dimensional molecular zippers (H. W. Kim, J. Jung, M. Han, S. Lim, K. Tamada, M. Hara, M. Kawai, Y. Kim, and Y. Kuk)
- (3) Two dimensional superstructure formation of fluorinated fullerene on Au(111) (T. K. Shimizu, J. Jung, T. Otani, Y.-K. Han, M. Kawai, and Y. Kim)
- (4) Density functional theory calculation for magnetism of Fe-Phthalocyanine molecules on Au(111) (E. Minamitani, D. Matsunaka, N. Tsukahara, N. Takagi, M. Kawai, and Y. Kim)

- Research plan for FY2011

- (1) Doping effect on H<sub>2</sub>O and O<sub>2</sub> dissociation on the metal supported oxide film surface.
- (2) Hopping of CO molecule on Ag(100) and MgO/Ag(100) surfaces
- (3) Adsorption of pi-conjugated molecules on the noble metal surfaces
- (4) Electronic structure of one-dimensional molecular assembly on the hydrogen terminated Si(100)
- (5) Electronic and magnetic states of Phthalocyanine molecules on surface
- (6) Analysis of Kondo effect in FePc/Au(111)
- (7) DFT-based STM simulation using NEGF

method

- (8) Electronic structure of graphene/Pt(111)

7 . If you have a “General User” account and could not complete your allocated computation time, specify the reason.

We have used about 70 % of the assigned CPU resources to us. The biggest reason is that many of plans were changed due to the natural disaster early 2011. Therefore, we had to reconsider research plans, i.e., computational and experimental schedules, during the fiscal year. Next fiscal year, we will more carefully submit both the computation time per one project and the number of project per one member for FY2012 based on more detailed research planning.

**Fiscal Year 2011 List of Publications Resulting from the Use of RICC**

\* The members registered as the user of RICC system in FY2011 are indicated by underline.

**[Publication]**

1. J. Jung, H.-J. Shin, Y. Kim, and M. Kawai, "Activation of ultrathin oxide film by interface defect for chemical reaction", *J. Am. Chem. Soc.*, **133**, 6142 (2011).
2. H. W. Kim, J. Jung, M. Han, S. Lim, K. Tamada, M. Hara, M. Kawai, Y. Kim, and Y. Kuk, One-dimensional molecular zippers, *J. Am. Chem. Soc.* **133**, 9236 (2011).
3. T. K. Shimizu<sup>§</sup>, J. Jung<sup>§</sup>, T. Otani, Y.-K. Han, M. Kawai, and Y. Kim, Two dimensional superstructure formation of fluorinated fullerene on Au(111): A scanning tunneling microscopy study, *ACS Nano*, DOI: 10.1021/nn300064x. [<sup>§</sup> equally contributing authors]
4. E. Minamitani, D. Matsunaka, N. Tsukahara, N. Takagi, M. Kawai, and Y. Kim, Density functional theory calculation for magnetism of Fe-Phthalocyanine molecules on Au(111), *e-J. Surf. Sci. Nanotech.*, in press.

**[Oral presentation at an international symposium]**

1. Y. Kim, "Mode-selective and state-selective chemistry of a single molecule with tunneling electrons", The 29th International Brand Ritchie Workshop (BRW2011) on Particle Penetration Phenomena and Excitations of Solids, Matsue, Shimane, Japan, May (2011).
2. Y. Kim, "Reaction control of a single molecule with tunneling electrons", The 5th International Conference on Science and Technology for Advanced Ceramics (STAC5), Yokohama, Japan, Jun. (2011).
3. Y. Kim, "Mode-selective and state selective chemistry of a single molecule with tunneling electrons", The New Frontiers of Low Temperature Physics (ULT 2011), Daejeon, Korea, Aug. (2011).
4. E. Minamitani, D. Matsunaka, N. Tsukahara, N. Takagi, M. Kawai, and Y. Kim, "Ab-initio calculation of magnetism of Fe-phthalocyanine molecules on Au(111) surface", The 28th European Conference on Surface Science (ECOSS-28), Wrocław, Poland, Aug.-Sep. (2011).
5. J. Jung, H.-J. Shin, Y. Kim, and M. Kawai, "Role of the interface in the chemical reactivity of ultrathin oxide film", The 7th Congress of the International Society for Theoretical Chemical Physics (ISTCP-7), Tokyo, Japan, Sep. (2011).
6. H. W. Kim, J. Jung, M. Han, S. Lim, K. Tamada, M. Hara, M. Kawai, Y. Kim, and Y. Kuk, "Molecular zippers", The 2011 Materials Research Society Fall Meeting, Boston, USA, Nov.-Dec. (2011).
7. Y. Kim, J. Jung, H.-J. Shin, and M. Kawai, "State-selective reaction on the ultrathin insulating films", The 2011 Materials Research Society Fall Meeting, Boston, USA, Nov.-Dec. (2011).
8. Y. Kim, H.-J. Shin, J. Jung, and M. Kawai, "State-selective control of water dissociation on an ultrathin MgO film with STM", The 6th International Symposium on Surface Science (ISSS-6),

RICC Usage Report for Fiscal Year 2011

Tokyo, Japan, Dec. (2011).

9. J. Jung, H.-J. Shin, Y. Kim, and M. Kawai, “Controlling chemical reactivity of ultrathin oxide film by interface manipulation”, The 6th International Symposium on Surface Science (ISSS-6), Tokyo, Japan, Dec. (2011).
10. T. K. Shimizu, J. Jung, T. Otani, H. Imada, M. Kawai, and Y. Kim, “Combined STM and non-contact AFM study of interfacial structure and electronic states of fluorinated fullerene monolayer on Au(111)”, The 6th International Symposium on Surface Science (ISSS-6), Tokyo, Japan, Dec. (2011).
11. Y. Kim, “Reaction control of a single molecule with tunneling electrons”, The 3rd Global COE International Symposium: Electronic Devices Innovation (EDIS 2011), Osaka, Japan, Dec. (2011).